

Effect of nanoclay reinforcement on tensile and tribo behaviour of Nylon 6

G. SRINATH, R. GNANAMOORTHY*

Department of Mechanical Engineering, Indian Institute of Technology Madras,
Chennai 600 036, India

E-mail: gmoorthy@iitm.ac.in

Polymer nanocomposites are particle-filled polymers in which at least one dimension of the dispersed particles is in the nanometer range. Dispersing nanosize particles in a polymer matrix induces superior mechanical properties compared to traditional macro fillers. Nanolevel reinforcement also affects the tribological properties and needs to be clearly understood before using in practical applications. Friction and wear characteristics of Nylon 6 nanocomposites under dry sliding conditions are reported in this paper. Nylon 6 with 5% organoclay was prepared by melt intercalation technique. The tensile behaviour is evaluated according to ASTM standards. A pin-on-disc type tribometer is used for evaluating the friction and wear behaviour. It is found that the Nylon 6 nanocomposites have superior tribological properties than unfilled polymer. Formation of uniform tenacious transfer layer by Nylon 6 nanocomposite on the counterface contributes to the reduction in coefficient of friction and specific wear rate. Nylon Nanocomposites exhibited high wear resistance compared with the neat Nylon.

© 2005 Springer Science + Business Media, Inc.

1. Introduction

Advanced polymer composites are replacing metals in many bearing and gear applications owing to its lightweight and economic fabrication. Polymers have poor mechanical strength compared with metals and are reinforced with fillers and fibres to improve the mechanical properties. Fibres or fillers ranging from few tens of microns to few millimetres of length are reinforced in commercial reinforced composites. If a nanometer level dispersion could be achieved, the mechanical properties might be further improved [1]. Layered polysilicate clays like montmorillonite, hectorite, and saponite are the few potential precursors used for producing nanolevel dispersion [2]. These clays have silicate layers held together by vanderwals bonds. Dispersion of the layers or agglomerated tactoids into discrete monolayers, which can be achieved by various methods including, melt intercalation, yields a new class of material called Polymer Clay Nanocomposite (PCN). Layered silicate clays are hydrophilic and are less suitable for mixing and interacting with most polymer matrices. These silicate clays are organically modified to make it compatible with organic matrix, which helps in better intercalation and exfoliation. Cho and Paul [3] prepared Nylon 6 nanocomposites by melt compounding using a conventional twin-screw extruder and found the mechanical properties of the nanocomposites were significantly increased with a marginal decrease in ductility. Addition of organoclay to Nylon 6

significantly increases the ductile-to-brittle transition temperature [3]. Nylon 11/organoclay nanocomposites prepared by melt compounding exhibited high thermal stability, storage modulus and tensile strength [4]. Polyamide 12/fluomica and polyamide 12/organically modified fluomica nanocomposites prepared by melt compounding technique exhibited superior mechanical properties compared with neat Nylon 12 [5].

Recent investigations reveal that the polymer nanocomposites also exhibit good tribological properties [6–8]. Friction and wear tests were conducted on low nanometer silicon nitride filled epoxy composites by Guang *et al.* [6]. The composite materials exhibit significantly improved tribological performance and mechanical properties at low filler content. Tribochemical reactions involving Si_3N_4 nanoparticles were accounted for the improved tribological performance of nano- Si_3N_4 /epoxy composites. Friction and wear properties of nanometer SiO_2 filled polyetheretherketone (PEEK) were studied by Wang *et al.* [7]. The nano sized SiO_2 filled PEEK showed considerably lower wear rate and coefficient of friction than neat PEEK. The improved performance was attributed to the formation of a thin, uniform tenacious transfer layer on the counterface. The wear resistance of nano sized ZnO filled PTFE increased while the coefficient of friction remained the same due to prevention of destruction of the PTFE banded structure during the friction process by nanometer ZnO [8].

*Author to whom all correspondence should be addressed.

Nylon 6 being a most common engineering thermoplastic is used in many tribological applications [9]. Nylon 6 nanocomposites have been successfully prepared and found to exhibit superior mechanical properties [3–5]. Tensile and tribological behaviour of organoclay reinforced Nylon 6 based composites are reported in this paper.

2. Materials and processing

Commercial grade Nylon 6 is used for preparing the nanocomposites. The organoclay used was montmorillonite modified by 2 methyl, 2 hydrogenated tallow quaternary ammonium chloride (Elementis Specialties, USA). Individual platelet size of the clay ranges from about $0.5 \times 0.5 \times 0.001$ microns to about $0.8 \times 0.8 \times 0.001$ microns in size while the clay bundles is of the order of about 75 microns [10].

Nylon 6 granules were preheated at 333 K for 4 h before extrusion. The organoclay was mixed with Nylon 6 pellets thoroughly using a screw mixer and fed into the twin-screw extruder (Make Berstroff). The extrudate was cooled by passing through a water bath and small pellets were made by using a chopper. The X ray diffraction analyses were conducted on the molded specimens to find out the dispersion of clay in nanocomposite.

Tensile specimens according to dimensions prescribed in ASTM D 638 [11] were injection molded to evaluate the tensile behaviour of Nylon 6 and Nylon 6 nanocomposite. Gage length and thickness of the tensile specimen are 7.62 and 4 mm respectively. Specimens were injection molded at a pressure of 125 MPa and at a temperature of 513 K. Tests were carried out according to ASTM D 638 using an Instron tensile testing machine. At least three tests were conducted in each material. Tests were performed at a constant strain rate of 2 mm/s at room temperature.

Tribological properties of test materials were studied using a pin-on-disc tribometer developed in the laboratory according to ASTM G99 [12]. Injection moulded cylindrical pins of 8 mm diameter and 20 mm length were used. The counter face disc was made of stainless steel (AISI 314). The centre line average surface roughness (R_a) of the ground disc is $0.6 \mu\text{m}$. The friction force was measured by using a force transducer fixed on the loading lever arm and the temperature of the disc was measured by using a non-contact infrared tem-

perature sensor (Fig. 1). Friction and wear tests were conducted at different normal loads varying from 30 to 60 N. Tests were performed at a constant sliding velocity of 0.4 m/s. Tests were conducted under unlubricated dry laboratory conditions ($32^\circ\text{C} \pm 3^\circ\text{C}$, RH $57\% \pm 5\%$). Friction force and disc temperature were measured continuously and data were stored using a personal computer based data acquisition system. The sliding surfaces of the pins were cleaned before testing. The initial mass of pins was measured using an electronic balance of 0.1 mg accuracy and the dimensions of pins were measured using a digital micrometer of accuracy $1 \mu\text{m}$. The centre line average surface roughness (R_a) of the pin and disc was measured using a perthometer. Tests were run up to a sliding distance until the coefficient of friction stabilises. After the test the pin was cleaned and the specimen mass and surface roughness were measured. Three tests were conducted under each test condition and the average values of measured friction force, disc temperature and mass loss were used for further analysis. The specific wear rate (K_o) was calculated using Equation 1

$$K_o = \frac{(m_1 - m_2) \times 1000}{\rho N S} \quad (1)$$

where m_1 and m_2 are mass (g) of specimen before and after testing, ρ is the specific gravity of the specimen, N is the normal load (N) and S is the sliding distance (m). The worn-out surfaces were observed using optical microscope.

3. Results and discussion

3.1. Clay exfoliation

Fig. 2 shows the X-ray diffraction patterns of organoclay and Nylon 6 nanocomposite. Organoclay shows a diffraction peak at 7.2° corresponding to the gallery spacing between the clay platelets. During melt processing the polymer molecule intercalates into the galleries of the clay and exfoliates the layers. Hence the gallery distance is not detected in the X-ray diffraction patterns of Nylon 6 nanocomposite.

3.2. Tensile behaviour

The typical stress-strain data of Nylon 6 and Nylon 6 nanocomposites are shown in Fig. 3. Tensile properties

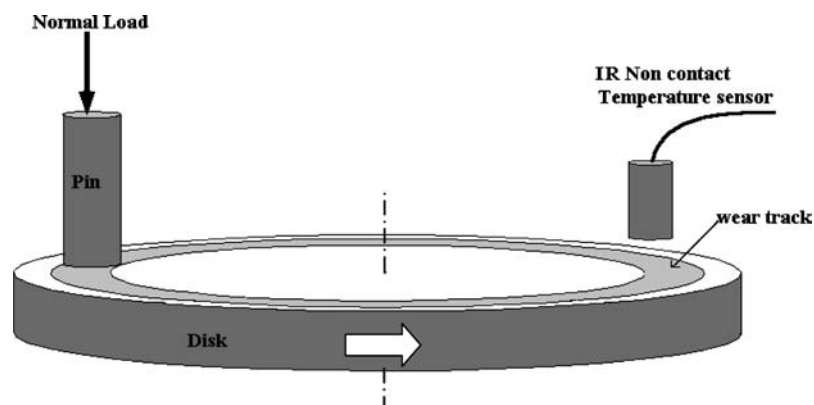


Figure 1 Schematic representation of pin-on-disc configuration.

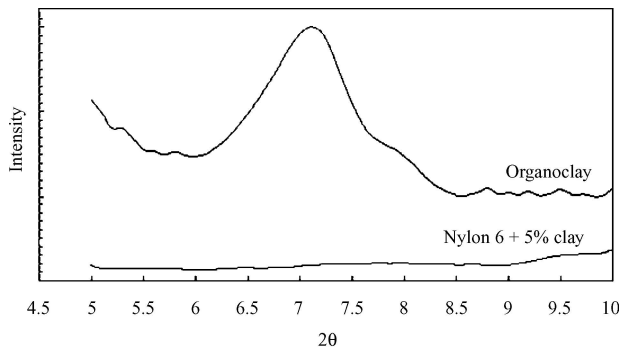


Figure 2 X-ray diffraction patterns of organoclay and Nylon 6 nanocomposite.

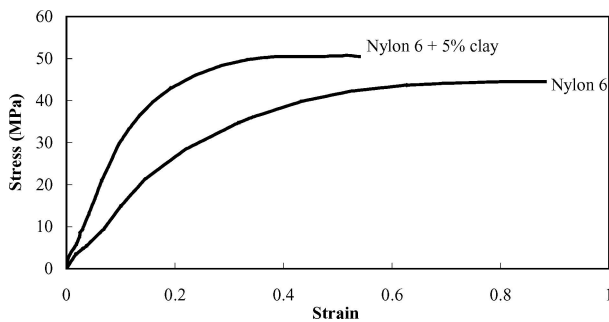


Figure 3 Stress-strain curves of Nylon 6 and Nylon nanocomposite.

derived from the curves are given in Table I. Nylon 6 nanocomposite exhibits higher tensile strength and tensile modulus than Nylon 6. Due to addition of 5% clay the tensile strength increases (by $\sim 14\%$) but there is a drastic improvement in Young's modulus (increased by 120%). The number of available reinforcing elements is increased due to dispersion of clay layers and it improves the load carrying capacity. As aspect ratio of clay is high, it has a large surface area available for adhesion between the polymer molecules and clay layers. This facilitates better load transfer to the reinforcing phase and contributes to the improved strength and modulus [2]. However the tensile property improvements occur sacrificing the ductility of the polymer similar to any other engineering material. The elongation at fracture decreases from 384 to 95%. Hence there is a decrease in toughness, measured by the area under stress-strain curve, and the elastic resilience, calculated by the area under the stress-strain curve up to elastic limit, indicating less energy required for fracture and deformation of nanocomposite than Nylon 6. Nano level reinforcement though improves the strength and modulus imparts brit-

TABLE I Tensile properties of Nylon 6 and Nylon 6 nanocomposite

Properties	Nylon 6	Nylon 6 + 5% clay
Ultimate tensile strength (MPa)	44.6 ($\pm 5\%$)	50.8 ($\pm 5\%$)
Yield strength (MPa)	30 ($\pm 5\%$)	21 ($\pm 5\%$)
Modulus (MPa)	145 ($\pm 10\%$)	315 ($\pm 10\%$)
Elongation at break	384% ($\pm 3\%$)	95% ($\pm 5\%$)
Area under stress strain curve (MPa)	30.3 ($\pm 5\%$)	22.1 ($\pm 5\%$)
Elastic resilience (MJ/m^3)	1.54 ($\pm 5\%$)	1.49 ($\pm 5\%$)

tleness to the composite. Similar results were reported in polyamide, PA 11 [4] and polypropylene [13] nanoclay systems. Liu *et al.* [4] observed similar improvements in the tensile strength and modulus sacrificing the ductility for PA 11 by reinforcing with organoclay. Addition of 4% organoclay shows significant improvement in tensile strength and modulus with drastic decrease in elongation at break. A decrease in the area under stress-strain curve due to 1% nano silica reinforcement in polypropylene with significant improvements in tensile strength and modulus was reported by Wu *et al.* [13].

3.3. Friction and wear behaviour

Owing to changes in the real area of contact and shear strength of polymer, in most sliding tests the run-in friction precedes the steady state friction [14]. A similar trend was observed in Nylon 6 and Nylon 6 nanocomposites during the current studies (Fig. 4). The coefficient of friction increases initially and then stabilizes after the initial run-in period. The effect of nano level reinforcement is evident as nanocomposites exhibits lower coefficient of friction than Nylon 6. The nano level reinforcement reduces the average steady state coefficient of friction from 0.50 to 0.35.

The effect of applied normal load on the coefficient of friction of Nylon 6 and Nylon 6 nanocomposites is shown in Figs 5 and 6. The coefficient of friction increases with increase in normal load due to the changes in the real area of contact [15]. Both the materials exhibit the similar trend. During injection moulding as polymer cools in the mould, a skin is formed over the surface [16, 17]. This skin is harder than the inside material. Table II shows the durometer hardness (Shore D) measured at moulded exterior surface and cut surface

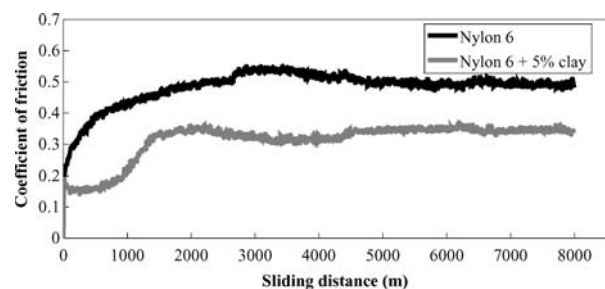


Figure 4 Effect of sliding distance on coefficient of friction at the normal load of 60 N and sliding speed of 0.4 m/s.

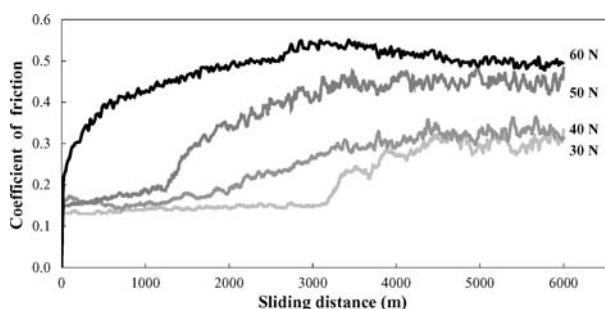


Figure 5 Variation of coefficient of friction for Nylon 6 at different normal loads (sliding speed = 0.4 m/s).

TABLE II Hardness (Shore D) of the pins

	Hardness (Shore D) of the pin	
	At moulded surface	At cut surface
Nylon 6 + 5% Clay	75	70
Nylon 6	72	68

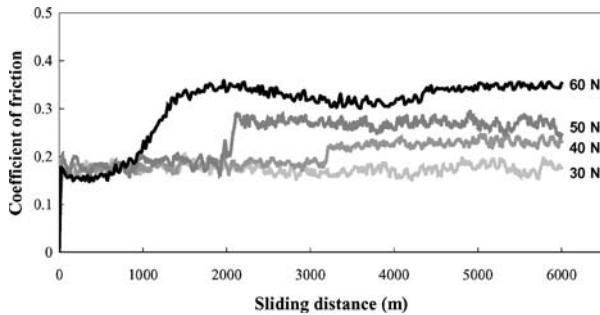


Figure 6 Effect of normal load on the coefficient of friction of Nylon 6 nanocomposites (sliding speed = 0.4 m/s).

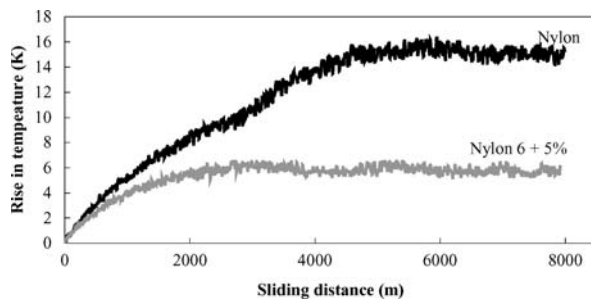


Figure 7 Temperature rise of the disc during the tests conducted at the normal load of 60 N and sliding speed of 0.4 m/s.

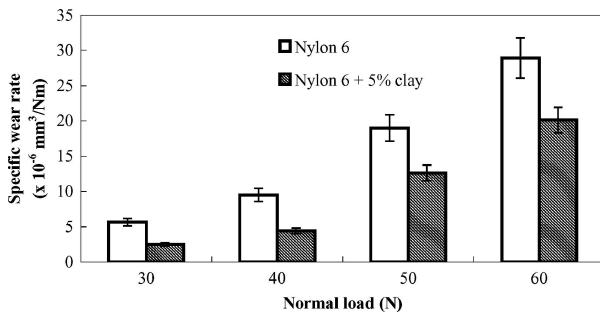


Figure 8 Effect of normal load on specific wear rate.

(inside material) of Nylon 6 and Nylon 6 nanocomposite. The changes in real area of contact and formation of transfer film in addition to the formation of skin influence the coefficient of friction. At lower loads, the coefficient of friction is low and after certain distance of sliding, the coefficient of friction increases and steadies off. Increase in the normal load also shifts the transition region (change from run-in friction to steady state friction) towards left, as the increase in applied load tends to disrupt the skin faster. At the applied normal load of 60 N, a complete shift of the transition region towards left was achieved for Nylon 6 but not in the nanocomposite. In Nylon 6 nanocomposite the skin is harder than the skin formed on pristine Nylon and hence requires a higher load to disrupt it. Nylon 6 nanocomposite specimens require a higher load to attain the complete shift of the transition region.

During the test, the rise in temperature of the disc was observed due to frictional heating [18]. Fig. 7 shows the rise in temperature of the disc during the sliding tests for tests conducted up to a distance of 8000 m at normal load of 50 N and sliding velocity of 0.4 m/s. A higher temperature rise was observed during tests with Nylon 6 pins compared with tests conducted with nanocomposite pins. As the coefficient of friction is high, when the Nylon 6 slides over the stainless steel the heat generated is also high. Similar results were also observed at all other loads investigated.

Effect of normal load on specific wear rate of Nylon 6 and Nylon 6 nanocomposite is shown in Fig. 8. Nylon 6 nanocomposite is more wear resistant than Nylon 6 at all normal loads investigated. The specific wear rate of both Nylon 6 and Nylon 6 nanocomposite increases with an increase in the normal load, as the wear loss is proportional to the normal load [19].

Nylon 6 nanocomposite with 5% clay exhibited a lower coefficient of friction and specific wear rate than pristine Nylon 6 at all test conditions investigated. This behavior may be attributed to interfacial strengthening of the nano level reinforcements [20, 21]. As the clay particles are dispersed in nano level in Nylon 6 matrix and also due to the high specific surface area of the nanoparticles the interfacial adhesion between matrix and nanoparticle is high and contributes to the improved tribological behavior. Due to the presence of

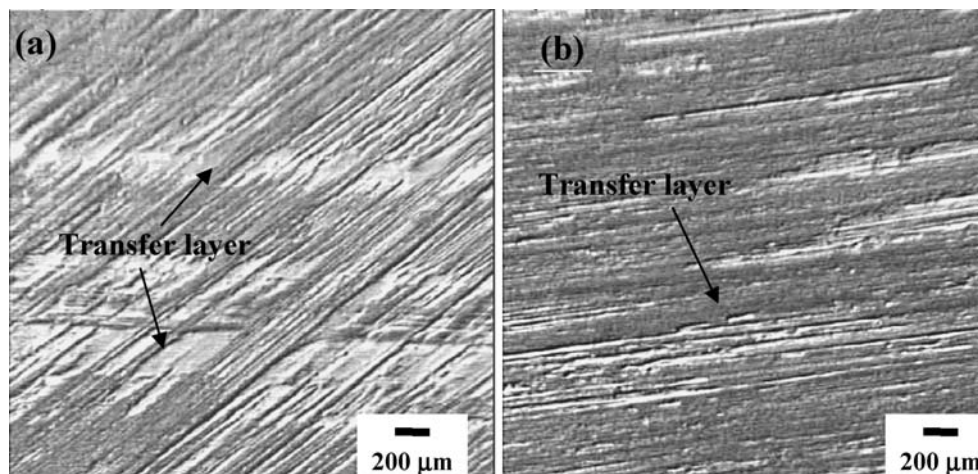


Figure 9 Transfer layer formed on the counterface disc after sliding at normal load 50 N and speed 0.4m/s of: (a) Nylon 6 and (b) Nylon 6 + 5% clay.

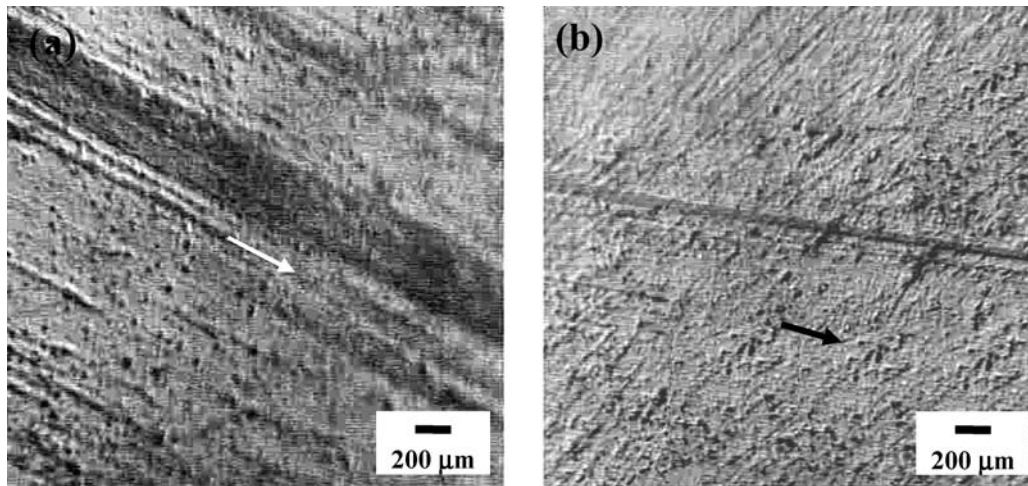


Figure 10 Worn pin surface after sliding at the normal load 50 N and speed 0.4 m/s of: (a) Nylon 6 and (b) Nylon 6 + 5% clay (arrow indicates the sliding direction).

nanolevel filler, which has the same size as the segments of the surrounding polymer chains, the material removal of nanocomposites is mild and also aids in the formation of uniform tenacious transfer layer [7, 22]. This is evident from the micrographs (Fig. 9a and b) of the transfer layer formed on the counterface. Fig. 9a shows the transfer layer formed on the counterface during sliding of Nylon 6 pins. The worn surfaces of Nylon 6 and Nylon 6 nanocomposite are shown in Fig. 10. Due to the formation of patchy incoherent transfer film on the counterface, the wear track formed during Nylon 6 pin is severe and thick. The wear tracks observed in the nanocomposite pin are thin due to protection offered by the transfer layer formed on the disc.

4. Conclusions

Tensile and tribo behaviour of Nylon 6 and Nylon 6 nanocomposite are investigated and the following conclusions were drawn:

1. Nylon 6 nanocomposite exhibit higher tensile strength and modulus than pristine Nylon 6.
2. Coefficient of friction of Nylon 6 nanocomposite under dry sliding conditions when slid against stainless steel was lesser than that of Nylon 6.
3. Nanolevel filler is effective in reducing the specific wear rate of Nylon 6 at all the normal loads investigated.
4. Formation of uniform tenacious transfer layer by Nylon 6 nanocomposite on the counterface contributes to the reduction in coefficient of friction and specific wear rate.
5. Presence of nanolevel filler of same size of the surrounding polymer molecules causes mild material removal.

Acknowledgment

The support for one of the authors from the Department of Science and Technology, Government of India, is gratefully acknowledged.

References

1. PETER C. LEBARON, ZHEN WANG and THOMAS J. PINNAVAIA, *Appl. Clay Sci.* **15** (1999) 11.

2. T. J. PINNAVAIA and G. W. BEALL, in "Polymer-Clay Nanocomposites" (John Wiley, 2001) p. 3.
3. J. W. CHO and D. R. PAUL, *Polymer* **42** (2001) 1083.
4. TIANXI LIU, KIAN PING LIM, WUIWUI CHAUHARI TJIU, K. P. PRAMODA and ZHI-KUAN CHEN, *ibid.* **44** (2003) 3529.
5. TONY MCNALLY, W. RAYMOND MURPHY, CHUN Y. LEW, ROBERT J. TURNER and GERARD P. BRENNAN, *ibid.* **44** (2003) 2761.
6. GUANG SHI, MING QIU ZHANG, MIN ZHI RONG, BERND WETZEL and KLAUS FRIEDRICH, *Wear* **254** (2003) 784.
7. QI-HUA WANG, JINFEN XU, WEICHANG SHEN and QUNJI XUE, *ibid.* **209** (1997) 316.
8. FEI LI, KE-AO HU, JIAN-LIN LI and BIN-YUAN ZHAO, *ibid.* **249** (2002) 877.
9. KEVIN S. MARSHALL, *Machine Design*. **Jan 10** (2002) 81.
10. BENTONE 105-Technical Information (Elementis Specialties Inc, Highstown, 2003).
11. ASTM D 638, "Standard Test Method for Tensile Properties of Plastics," Vol. 8.01 (ASTM International, West Conshohocken, 2002) p. 45.
12. ASTM G99, "Standard Test Method for Wear Testing with a Pin-on-Disc Apparatus", (ASTM International, West Conshohocken, 2002) p. 414, Vol. 3.02.
13. CHUN LEI WU, MING QIU ZHANG, MIN ZHI RONG and KLAUS FRIEDRICH, *Comp. Sci. Tech.* **62** (2002) 1327.
14. SHIN JEN SHIAO and TE ZEI WANG, *Composites* **27B** (1996) 459.
15. DESMOND F. MOORE, in "Principles and Application of Tribology" (Pergamon Press, Oxford, 1975) p. 61.
16. KYE-CHYN HO and MING-CHANG JENG, *Wear* **206** (1997) 60.
17. DOMINICK V ROSATO and DONALD V ROSATO, in "Plastics Engineering Product Design" (Elsevier, Oxford, 2003) p. 106.
18. SURJEET K. SINHA, in "Wear Failure of Plastics," ASM Handbook, Vol. 11 Failure Analysis and Prevention, edited by William T. Becker and Roch J. Shipley (ASM International, Ohio, 2002) p. 1020.
19. I. M. HUTCHINGS, in "Tribology: Friction and Wear of Engineering Materials" (Edward Arnold, London, 1992) p. 129.
20. HUI CAI, FENGYUAN YAN, QUNJI XUE and WEIMIN LIU, *Polym. Test.* **22** (2003) 875.
21. GUANG SHI, MING QIU ZHANG, MIN ZHI RONG, BERND WETZEL and KLAUS FRIEDRICH, *Wear* **256** (2004) 1072.
22. CHRISTIAN J. SHWARTZ and SHYAM BHADUR, *ibid.* **237** (2000) 261.

Received 19 June 2003

and accepted 25 August 2004